Available online at www.sciencedirect.com
SCIENCE DIRECT®
Virology 318 (2004) 192–203
VIROLOGY
www.elsevier.com/locate/yviro

The refined structure of *Nudaurelia capensis* ω Virus reveals control elements for a $T = 4$ capsid maturation

Charlotte Helgstrand,[a] Sanjeev Munshi,[b] John E. Johnson,[c] and Lars Liljas[a,*]

[a] *Department of Cell and Molecular Biology, Uppsala University, Box 596, 751 24 Uppsala, Sweden*
[b] *Merck Research Laboratory, Lansdale, PA 19486, USA*
[c] *Department of Molecular Biology, The Scripps Research Institute, La Jolla, CA 92037, USA*

Received 15 August 2003; accepted 25 August 2003

Abstract

Large-scale reorganization of protein interactions characterizes many biological processes, yet few systems are accessible to biophysical studies that display this property. The capsid protein of *Nudaurelia capensis* ω Virus (NωV) has previously been characterized in two dramatically different $T = 4$ quasi-equivalent assembly states when expressed as virus-like particles (VLPs) in a baculovirus system. The procapsid (pH 7), is round, porous, and approximately 450 Å in diameter. It converts, in vitro, to the capsid form at pH 5 and the capsid is sealed shut, shaped like an icosahedron, has a maximum diameter of 410 Å and undergoes an autocatalytic cleavage at residue 570. Residues 571–644, the γ peptide, remain associated with the particle and are partially ordered. The interconversion of these states has been previously studied by solution X-ray scattering, electron cryo microscopy (CryoEM), and site-directed mutagenesis. The particle structures appear equivalent in authentic virions and the low pH form of the expressed and assembled protein. Previously, and before the discovery of the multiple morphological forms of the VLPs, we reported the X-ray structure of authentic NωV at 2.8 Å resolution. These coordinates defined the fold of the protein but were not refined at the time because of technical issues associated with the approximately 2.5 million reflection data set. We now report the refined, authentic virus structure that has added 29 residues to the original model and allows the description of the chemistry of molecular switching for $T = 4$ capsid formation and the multiple morphological forms. The amino and carboxy termini are internal, predominantly helical, and disordered to different degrees in the four structurally independent subunits; however, the refined structure shows significantly more ordered residues in this region, particularly at the amino end of the B subunit that is now seen to invade space occupied by the A subunits. These additional residues revealed a previously unnoticed strong interaction between the pentameric, γ peptide helices of the A and B subunits that are largely proximal to the quasi-6-fold axes. One C-terminal helix is ordered in the C and D subunits and stabilizes a flat interaction in two interfaces between the protein monomers while the other, quasi-equivalent, interactions are bent. As this helix is arginine rich, the comparable, disordered region in the A and B subunits probably interacts with RNA. One of the subunit–subunit interfaces has an unusual arrangement of carboxylate side chains. Based on this observation, we propose a mechanism for the control of the pH-dependent transitions of the virus particle.

Keywords: Virus assembly; Quasi-equivalence; Tetraviruses; Nodaviruses; Disorder

Introduction

The *Nudaurelia capensis* ω Virus (NωV) is a member of the Tetraviridae family, which infects insects of the lepidopteran order (butterflies and moths). The capsid consists of 240 copies of a single protein type, arranged in four unique structural environments to form a $T = 4$ quasi-equivalent icosahedral surface lattice. While many virus families have capsids with $T = 3$ symmetry, only a few have $T = 4$ symmetry. The other high-resolution structure of a $T = 4$ capsid is that of the hepatitis B virus (HBV α) core (Wynne et al., 1999). When the NωV structure was determined (Munshi et al., 1996), it was obvious that the fold was very similar to the known structures of two other insect viruses, black beetle virus (BBV) (Hosur et al., 1987; Wery et al., 1994) and Flock House virus (FHV) (Fisher and Johnson, 1993), belonging to the $T = 3$ Nodaviridae family. Both families undergo a maturation process involving an autoproteolytic cleavage, and the cleavage sites are very similar. Although no significant sequence similarity is found between the capsid proteins of NωV and the nodaviruses

* Corresponding author. Fax: +46-18-536971.
E-mail address: lars@xray.bmc.uu.se (L. Liljas).

0042-6822/$ - see front matter © 2003 Elsevier Inc. All rights reserved.
doi:10.1016/j.virol.2003.08.045

BBV and FHV (the level of sequence identity is about 12%), the fold of the capsid proteins is similar, suggesting an evolutionary relationship between these virus groups.

Subsequent to the structure determination of the authentic NωV, a variety of biophysical studies were performed on $T = 4$ particles formed when the capsid protein was expressed in a recombinant baculovirus system. The form of NωV virus-like particles (VLPs) purified at pH 7 is called the procapsid, and is round and porous with a diameter of 450 Å. Quasi-symmetric subunit contacts are closely similar in the procapsid state, but the particles are only moderately stable (Canady et al., 2000). At pH 5, the particle is called the capsid and has a diameter is 410 Å and it is icosahedral in shape. Reorganization of an interior α-helical domain and translation and rotation of the subunits as rigid bodies differentiate quasi-symmetric contacts into two types of quasi-2-fold interactions, flat and bent. This capsid quaternary structure leads to an autoproteolytic cleavage at residue 570 (Taylor et al., 2002). After cleavage of at least 15% of the protein subunits, the conformational changes are irreversible in the wild-type capsid (Canady et al., 2000). An Asn570T hr cleavage-defective mutant, however, formed a capsid that could be reverted to the procapsid conformation when transferred to higher pH (Taylor et al., 2002).

We now report the refined structure of NωV at 2.8 Å resolution and describe, in chemical detail, the molecular switching that occurs in the helical domains that differentiates the four structural environments of the surface lattice. We can now also propose a mechanism for the pH-dependent transitions and discuss the significant differences in the arrangement of the γ peptides in nodaviruses and tetraviruses.

Results and discussion

Model building and refinement

The preliminary model (Munshi et al., 1996) was improved by reorienting several peptide bonds and side chains. In a few places in the helical domain, the main chain was extensively remodeled. When a mask extending 7 Å from the model atoms was used, it became evident that several new stretches of polypeptide could be modeled. In some locations, electron density for water molecules could be seen, and about 500 water molecules were included in the refined structure. A peak of electron density at a level similar to the protein was identified as a divalent metal ion by the nature of its ligands (aspartate side chains and carbonyl oxygens) and the ion to ligand distance (2.2–2.5 Å). There is no density at the inner surface of the protein shell that can reliably be attributed to the RNA. The final R value for about 2.5 million reflections and a model containing 2277 residues after temperature factor refinement is 22.0%. The final model has 1% of the residues in the disallowed and generously allowed regions of the Ramachandran plot as defined by PROCHECK (Laskowski et al., 1993). The refinement statistics are shown in Table 1.

Organization of the T = 4 virus capsid

The 240-protein monomers are arranged with $T = 4$ symmetry in the virus shell. The four quasi-equivalent conformations of the capsid protein are denoted A, B, C, and D. The shell can be viewed as constructed from two different types of trimers, ABC and DDD (Fig. 1a). ABC trimers surround each icosahedral 5-fold axis and the DDD trimers fill out the space between them, at the icosahedral 3-fold axes. Three ABC trimers and one DDD trimer form one face of the icosahedron. The DDD trimers follow icosahedral 3-fold symmetry, but the ABC trimers are related by a quasi-3-fold axis. In the $T = 4$ arrangement, two copies of three subunits (BCD) are adjacent to the icosahedral 2-fold axis, making it a quasi-6-fold. There are two unique quasi-2-fold axes, one relating two quasi-6-fold axes and the other relating a 5-fold axis and a quasi-6-fold axis (Fig. 1a).

The fold of the NωV capsid protein is an elaboration of the canonical viral jellyroll (Fig. 2). The standard viral jellyroll has eight anti-parallel β strands named from B to I and the loops connecting each strand are named BC, CD, etc. In NωV, this motif is modified by extensive insertions at the N- and C-termini as well as in several of the loops connecting the β strands. The N- and C-termini are only partly ordered, and the degree of order differs among the subunits. The N-terminal 40 amino acids are disordered in all subunits. This segment contains 10 arginine and 2 lysine residues and is probably associated with the RNA molecules. At the visible N-terminus, there are up to four helices, αN1–αN4 and at the C-terminus, there are up to four helices, αC1–αC4. The helices from both termini of one subunit have close approaches with each other and interact extensively with helices from symmetry-related subunits forming a modular, internal, ‘‘helical domain’’ that is

Table 1
Statistics from model building and refinement

R factor[a] (%)	22.0
Rms deviation of	
Bond lengths (Å)	0.007
Bond angles (deg)	1.4
Dihedral angles (deg)	25.4
Improper angles (deg)	0.83
Average B factor of	
Protein (Å^2)	28
Mg^{2+} (Å^2)	24
H_2O (Å^2)	30
Ramachandran outliers[b] (%)	0.7 + 0.2
Ramachandran outliers[c] (%)	4.0

[a] R factor $= \sum \| F_{obs} | - k | F_{calc} \| / \sum | F_{obs} |$, summation over all hkl for all reflections in the working set, no cut-off was used.
[b] Ramachandran outliers in generously allowed and disallowed regions defined according to Procheck (Laskowski et al., 1993).
[c] Ramachandran outliers regions defined according Moleman (Kleywegt and Jones, 1996).

spatially separate from the β-sandwich domains that form the shell.

An insertion in the CD loop adds two additional strands, βC′ and βC to one of the sheets in the jellyroll motif, as well as three helices, αCD1–αCD3. A large insertion in the EF loop forms a complete immunoglobulin-like (Ig-like) domain (101 residues) that protrudes on the outer surface of the virus particle. Before and after the Ig domain, there are two strands, βE′ and βE, which are antiparallel and form a small β-sheet together with a strand, βG′, from an insertion in the GH loop.

The A, B, C, and D subunits all have slightly different conformations (Fig. 2). The differences are mostly in the internal, α-helical domain, but the BC loop has two types of conformations, one in A and B and another in C and D. Subunits C and D are very similar in the helical domain, while A and B have their own distinct arrangements. The secondary structure assignment for each subunit is shown in Fig. 3.

The NωV structure is remarkably similar to that of BBV. Except for the Ig domain and a few loop regions, the structures superimpose very well. The rms deviations after superposition for the A, B, and C subunits of NωV and BBV (including the γ peptides) are 1.7–1.8 Å for about 230 atoms using the default cutoff in O (Jones et al., 1991). The regions that superimpose well and are used for the RMSD calculation include the eight strands in the viral jellyroll (βB–βI), βC′, βC, αN3, αC1, and the region close to the cleavage (Fig. 2).

In the same way as in several $T = 3$ viruses, the quasi-2-fold as well as the 5-fold and quasi-6-fold subunit interactions of NωV can be described as having two states, a flat or a bent contact. The same portions of the subunits are juxtaposed in these contacts, but the residues interacting are remarkably different with only those along a hinge maintained. The dihedral angle between subunits at the flat contact is 180° and it is 144° at the bent contact. The contacts between A subunits at the 5-fold axes, between B and C at the quasi-6-fold axes and between A and B at the quasi-2-fold axes are bent (Fig. 1). The quasi-6-fold contacts between B and D and between C and D, and the quasi-2-fold between C and D, are flat (Fig. 1). The difference in conformation is due to the insertion of C-terminal helices below the hinge at the flat contacts. This part is disordered in subunits A and B, but forms helix αC4 in C and D (Fig. 2). This helix is inserted as a wedge between the proteins in the BD and CD quasi-6-fold contacts (Fig. 4). The arrangement of the αC4 helices in the shell can be viewed in Fig. 1b. The large-scale effect is that the interactions between DDD trimers and ABC trimers are flat and interactions between different ABC trimers are bent.

Overall, the arrangement of the subunits in NωV is also very similar to that of the $T = 3$ insect viruses. When the ABC trimers of NωV and BBV are superimposed as rigid bodies, the rms deviation is 2.0 Å, only slightly higher than when the individual subunits are compared. The same type of quasi-2-fold, quasi-2-fold, 5-fold, and quasi-6-fold contacts that are present in NωV are also used in the $T = 3$ capsids. The most notable difference is that in the $T = 3$ packing, the icosahedral 3-fold axis is the quasi-6-fold, while in $T = 4$, the icosahedral 2-fold axis is the quasi-6-fold. At the atomic level, however, there is very little similarity in the subunit-subunit interactions. The coat proteins of nodaviruses have flat and bent contacts in the same way as in NωV, but the flat contacts are stabilized by an extended N-terminal segment from one of the subunits and by a segment of ordered double-stranded RNA (Fisher and Johnson, 1993; Tang et al., 2001).

Detailed interactions in the shell and molecular switching

The surface area of the coat protein that is buried when the capsid is formed is 1500–1700 $Å^2$ for the trimeric contacts, about 1400 $Å^2$ for the quasi-2-fold contacts, and 700–1200 $Å^2$ for the 5-fold and quasi-6-fold contacts. Of this surface area, the contacts involving the helical domains dominate the quasi-2-fold contacts and contribute 500–700 $Å^2$ to the 3-fold and quasi-3-fold contacts. The differences in contact area between the quasi-equivalent contacts are due to the differences between the flat and bent contacts and the different degree of order in the helical domain. The contact surfaces have a mixed polar and nonpolar character, but a large fraction of the quasi-2-fold contact is due to nonpolar contact between the helical domains. Some ordered water molecules are found in the subunit interfaces, but a large fraction of the waters are found in the space between the jellyroll and immunoglobulin domains.

The quasi 2-fold interactions are remarkably symmetric (Table 2). There are two types of quasi-2-fold dimers, AB and CD (Fig. 1a). The AB dimer has a bent conformation while the CD dimer is flat. Only one interaction is conserved between the two types of dimers and that is a "hinge" contact between Gln538 and Trp526. At the AB dimer interface, there is an unusual concentration of negative charges in close proximity (Fig. 5). The possible role of this contact in the control of maturation of the capsids is discussed below.

The interactions at the icosahedral 3-fold axis, between three D subunits, and at the quasi-3-fold axis, between A, B, and C subunits, are similar (Table 2, Figs. 6a–d). A large fraction of the 3-fold and quasi-3-fold contacts are between the external immunoglobulin domains and there the similarity is striking. The contacts in the interior helical domain are more different. Here, the contacts involve the ordered part of the N-termini, which differs in conformation and degree of order between the subunits, interacting with the γ peptide.

The AA, BC, CD, and DB interactions around the 5- and quasi-6-fold axes are quasi-equivalent to each other. Because of the difference in the interaction angle, however,

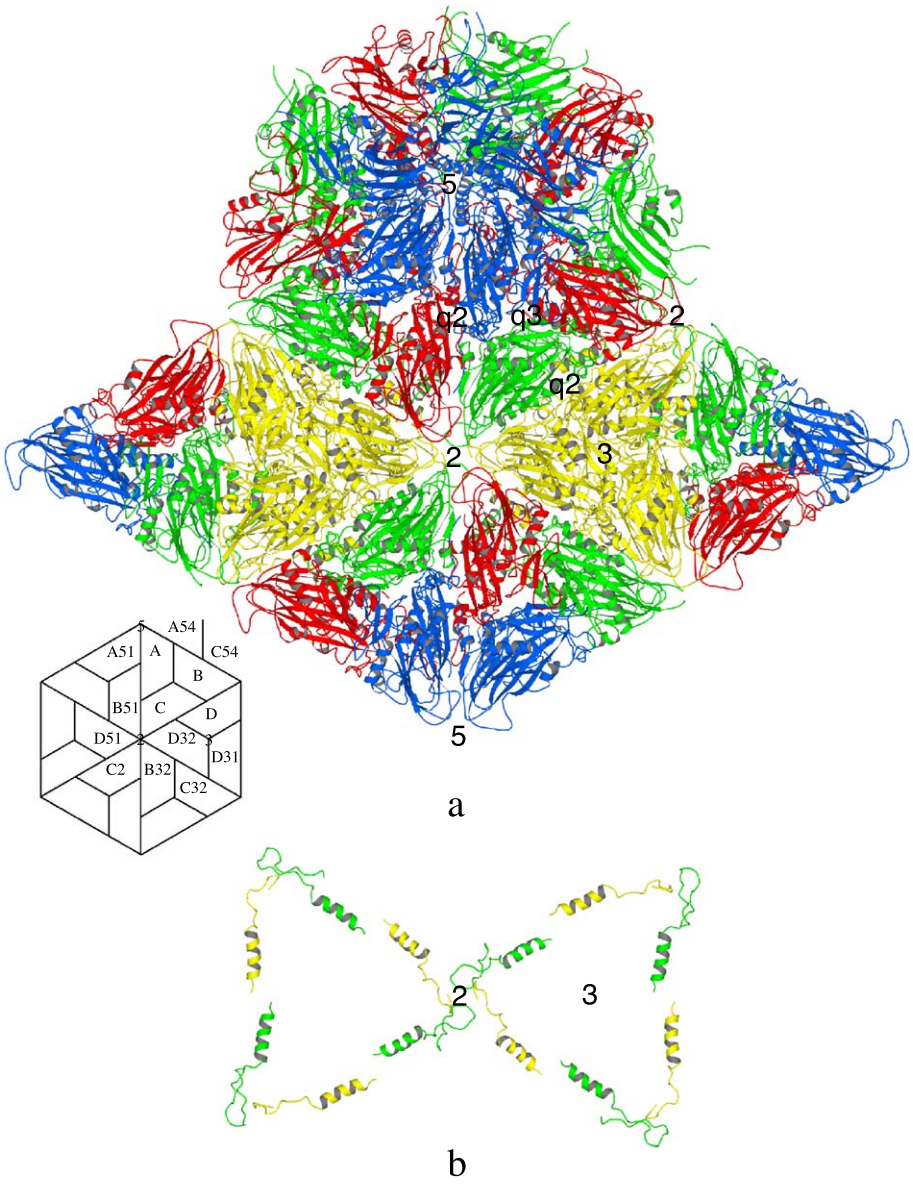

Fig. 1. (a) Schematic drawing of the NωV coat protein showing the $T = 4$ arrangement of the protein subunits in the shell. The immunoglobulin domain is omitted. A subunits are blue, B subunits are red, C subunits are green, and D subunits are yellow. This color scheme is used in all figures except Fig. 2. The symmetry and quasi-symmetry axes are marked. (b) The arrangement of the αC4 helices from the C and D subunits on the inside of the capsid in the same view as shown in a. Each DDD trimer is surrounded by a triangle of helices. A schematic view of the packing showing the denotation used in Table 2 is inserted. All schematic figures were made using the program Molscript (Kraulis, 1991).

only a few contacts are conserved between all subunits (Table 2). The interactions in the two bent contacts are very similar, as are the ones in the two flat contacts. The most striking differences are found in the interactions of the helical domains, including the cleaved γ peptides. It was previously reported (Munshi et al., 1996) that the γ peptides from the A subunit (αC2) formed a cylinder structure of five helices around the 5-fold axis. With the new polypeptides segments added, it became clear that there is instead a cylinder of 10 helices, which also includes the αN1 helices from B subunits (Figs. 7a and b). The αC2 helices are almost parallel to the axis, while the shorter αN1 helices are slightly tilted.

At the 2-fold (or quasi-6-fold) axis, the interactions are very different (Figs. 7c and d). The γ peptides of subunits C and D form three shorter helices, αC2–αC4, which all face the quasi-6-fold axes. One of these helices, αC4, acts as the wedge that forms the flat dimer interface. The conformation of the helices in subunits C and D is mostly similar but different from the conformation of the equivalent residues in the A subunits. In subunit A, αC2 is formed by residues 574–596, but in C and D, this helix consists of only residues 574–586. In C and D, the short helix αC3 (residues 594–598) is packed antiparallel to αC2 and is followed by a long, partly ordered, loop and helix αC4 (Fig. 2). The C-terminus of the B subunit is largely disordered and only a

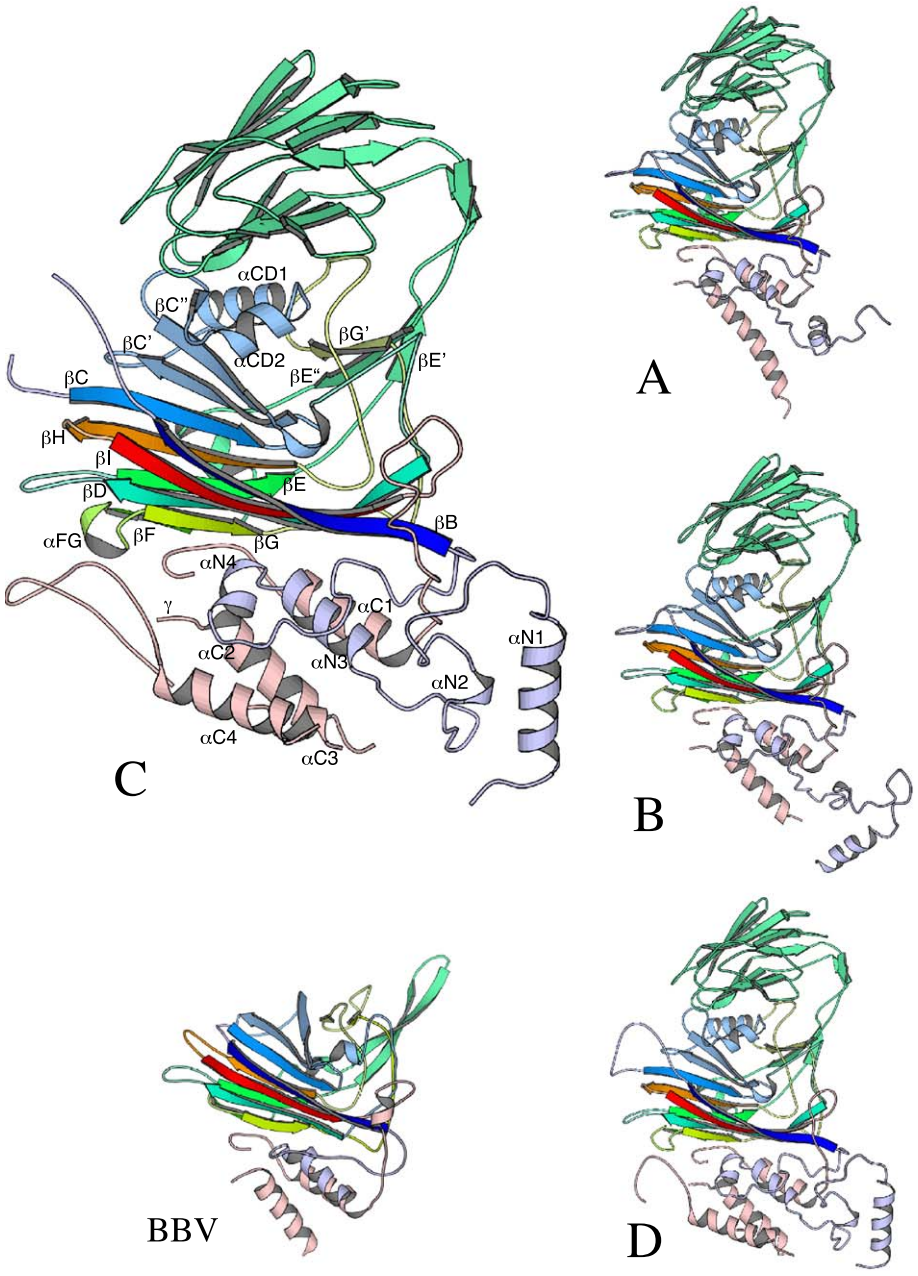

Fig. 2. The fold of the NωV monomer. All subunits A–D are shown, but the strands and helices are labeled in the C subunit only. The B subunit of black beetle virus (BBV) is included for a comparison. The standard viral jellyroll is shown in dark colors and the rest of the molecule is shown in pale colors. The N-terminus is pale blue, the C-terminus is pink, the CD loop is pale blue, the EF loop is pale green, and the GH loop is yellow. The helices αC2–αC4 are the visible part of the γ peptides.

short αC2 is visible and this faces the quasi-6-fold. At the flat contact, between subunits B and D, and between subunits D and C, the N-terminal helices (αN1) from D and C subunits are positioned between the γ peptide helices, in a way that resembles the arrangement around the 5-fold axis. At the bent contact, the corresponding element is the αN1 helix from the A subunit, but it is disordered because there is inadequate space for it. The four visible αN1 helices are roughly parallel to the quasi-6-fold axis, while all other helices are at an angle to the axis.

The helix αC4 has an exceptionally high arginine content: there are eight arginines in the segment 628–640 of the γ peptide. Segments of the coat protein rich in positively charged residues are found in many virus subunit sequences, but these segments are most often not visible in the electron density maps and presumed to be interacting with the viral nucleic acid. In NωV, this segment has a dual role. In the A and B subunits, it is disordered and available for interaction with the RNA molecules, but in the C and D subunits, it is ordered and used to stabilize the flat contact. Two of the

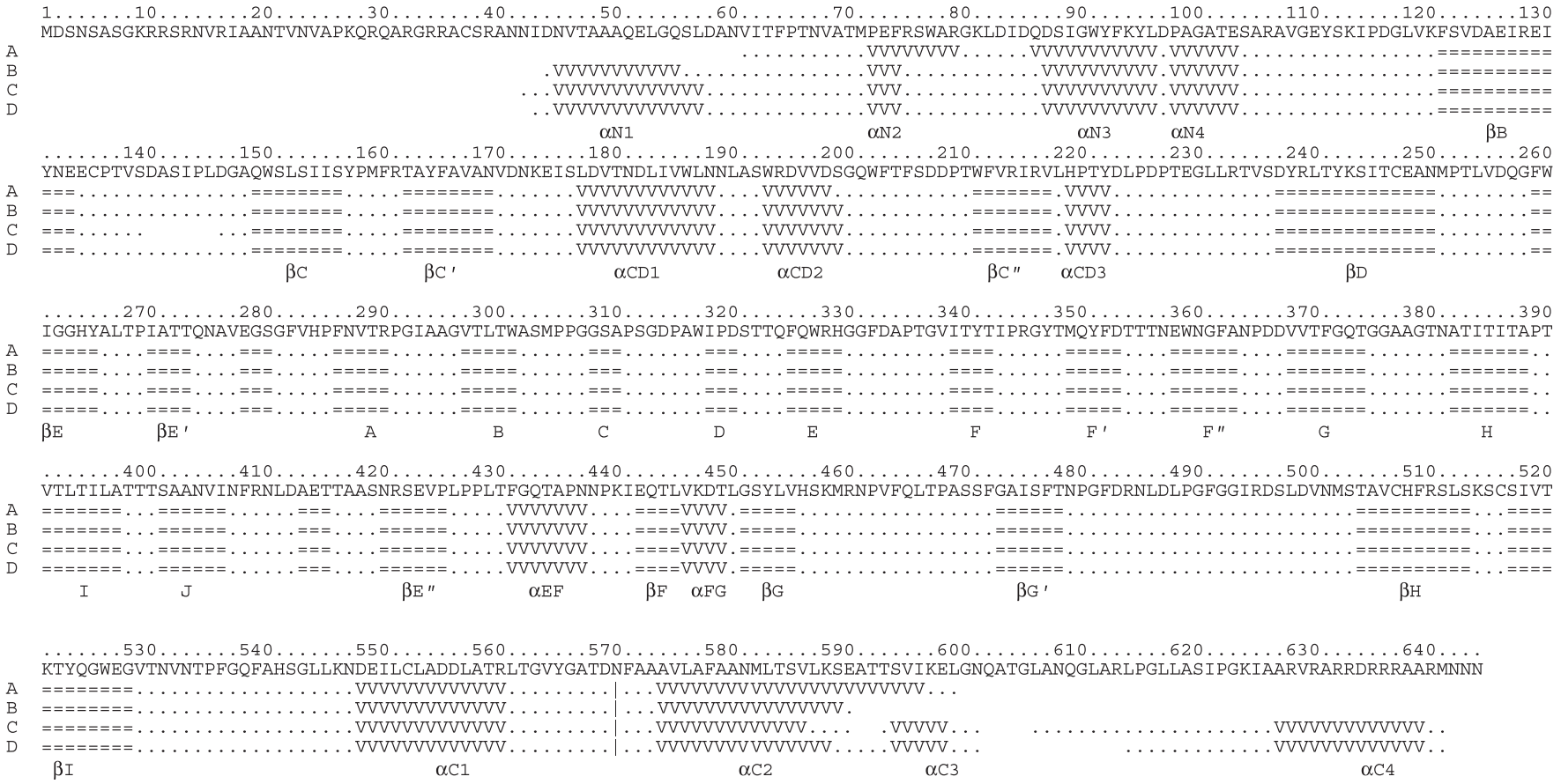

Fig. 3. The secondary structure assignment of each chain, aligned with the amino acid sequence. Helices are denoted by a "V" and strands with a "=".

Table 2
Polar interactions between subunits

Atom 1			Atom 2			A	B	C	D
Atom	Res	SSE	Atom	Res	SSE	A51	C54	D32	B
5,q6									
O	A 105	N4B	NH1	A51 560	αC1	2.9	–	–	–
O	B 105		NE	C54 560		–	3.1	–	–
O	A 106	N4B	NH1	A51 560		3.2	–	–	–
NH1	A 128	βB	O	A51 435	αEF	2.7	2.8	–	–
NH1	B 128		O	C54 436	αEF	–	3.0	–	–
OE1	C 129	βB	O	D32 432	αEF	–	–	2.5	2.6
O	C 132	βB	NH1	D32 510	βH	–	–	2.8	–
O	D 132		NH2	B 510		–	–	–	2.8
ND2	C 132		OG	D32 511	βH	–	–	2.9	3.0
O	A 140	BC	NE2	A51 149	βC	2.8	2.9	0	–
O	A 140		ND2	A51 172	C′CD1	2.8	2.8	0	–
O	A 141	BC	N	A51 149	βC	3.1	3.0	0	–
N	A 143	BC	O	A51 147	BC	2.8	3.0	0	–
OD1	C 146	BC	N	D32 146	BC	–	–	2.9	–
N	C 147	BC	OD1	D32 146	BC	–	–	2.8	–
NE2	C 201	CD2C″	O	D32 174	C′CD1	–	–	2.8	3.0
NH2	C 216	C″	OE2	D32 174	C′CD1	–	–	2.8	2.5
OD2	C 223	CD3D	NE2	D32 433	αEF	–	–	3.1	3.2
OE2	A 248	βD	NE2	A51 443	βF	2.7	2.7	–	–
OD1	A 250	βD	N	A51 258	DE	2.7	2.8	2.7	2.8
O	A 251	DE	NZ	A51 447	αFG	3.0	3.2	3.0	2.9
N	A 253	DE	OD1	A51 256	DE	2.8	2.8	2.9	2.8
OG1	A 253		OD2	C54 256		2.6	2.7	3.0	2.6
			NZ	A51 447	αFG	3.2	3.1	–	3.2
O	C 330	Im	OD1	D32 182	αCD1	–	–	Mg^{2+}	Mg^{2+}
			OD1	D32 207	CD2C″	–	–	Mg^{2+}	Mg^{2+}
OG1	D 336	Im	ND2	B 357	Im	–	–	–	2.6
OG	C 517	βI	OG	D32 511	βH	–	–	2.6	2.7
NZ	A 521	βI	O	A51 443	βF	2.7	2.8	–	–
			OE1	A51 443		–	–	2.9	–
N	C 612	C3C4	O	D32 616	C3C4	0	0	2.8	0
O	C 612		N	D32 618	C3C4	0	0	2.9	0
NE	C 613	C3C4	OD1	D32 256	DE	0	0	3.0	0
NZ	C 624	C3C4	OD2	D32 448	αFG	0	0	2.8	2.8
q2						B51	A54	D	C
OE1	C 51	αN1	NE	D 635	αC4	0	0	2.9	2.8
OE1	C 52	αN1	NE	D 628	αC4	0	0	3.1	–
			NH2	D 628		0	0	–	3.1
O	C 55	αN1	NH1	D 630	αC4	0	0	2.8	2.8
OD1	C 60	N1N2	NZ	D 624	C3C4	0	0	2.7	2.9
OG1	A 63	N1N2	O	B51 572	C1C2	3.0	2.9	–	–
OD1	A 87	αN3	OD2	B51 87	αN3	2.5	2.5	–	–
NH2	A 106	N4B	OD1	B51 60	N1N2	2.7	0	–	–
OE1	A 110	N4B	ND1	B51 541	IC1	3.0	3.0	–	–
OG	A 112	N4B	NE2	B51 541		3.0	3.2	–	–
OD1	B 124	βB	NE2	A54 541		–	3.2	–	–
N	A 126	βB	O	B51 538	IC1	3.1	2.9	–	–
OH	C 523	βI	O	D 62	N1N2	–	–	2.8	2.6
OE1	A 538	IC1	NE1	B51 526	βI	3.0	3.1	3.1	3.1
OD1	A 581	αC2	N	B51 60	N1N2	2.7	0	–	–
ND2	A581		O	B51 60		3.1	0	–	–
3,q3						B	C	A	D31
O	A 266	EE′	OG	B 236	CD	2.6	2.5	2.9	2.9
OG1	A 268	EE′	OD2	B 237	CD	2.5	2.5	2.5	2.4
O	A 271	βE′	ND2	B 420	βE″	3.1	3.0	3.1	3.0
O	A 280	Im	N	B 280	Im	–	3.1	–	–
			OG	B 280	Im	2.8	–	3.1	3.0
N	A 283	Im	OE2	B 278	Im	3.1	3.0	3.2	2.8
O	A 356	Im	NH1	B 345	Im	3.2	–	2.6	2.7
O	A 357	Im	NH1	B 345	Im	3.0	3.1	–	–

Table 2 *(continued)*

Atom 1			Atom 2			A	B	C	D
Atom	Res	SSE	Atom	Res	SSE	A51	C54	D32	B
OE2	B 358	Im	NE	C 345	Im	–	3.1	3.2	–
O	A 426	E′EF	ND2	B 531	IC1	2.9	2.9	3.1	2.9
OE1	A 433	αEF	N	B 533	IC1	2.6	2.8	2.6	2.9
O	A 437	αEF	OG1	B 530	IC1	2.6	2.7	2.7	2.6
NZ	A 440	EFF	O	B 120	N4B	2.8	–	3.0	2.9
OE2	B 442	βF	O	C 57	αN1	–	2.6	0	2.6
N	B 443	βF	O	C 60	N1N2	–	2.8	0	2.9
NE2	B 443	βF	O	C 60		–	2.9	0	2.9
O	A 460	GH	N	B 466	GH	3.1	3.2	3.2	–
OD1	A 461	GH	NE2	B 461	GH	Wat	Wat	Wat	Wat
NH2	A 484	GH	O	B 418	EF	3.0	3.1	3.1	3.0
OD1	A 485	GH	N	B 417	EF	3.0	3.1	3.0	2.9
OD2	B 555	αC1	NZ	C 546	IC1	–	3.1	–	–
OD1	A 556	αC1	N	B 546		3.2	3.1	3.2	3.0
O	A 558	αC1	NZ	B 120	N4B	2.9	2.8	2.9	2.7
OG1	A 559	αC1	O	B 117	N4B	3.2	3.0	3.0	3.0
NE	A 560	αC1	OE2	B 73	αN2	2.8	–	–	3.1
NH1	B 560		OE2	C 73		–	2.9	2.7	–
NH2	A 560		OD2	B 58		–	2.3	0	2.6
			OE2	B 73	αN2	2.9	–	–	3.1
O	A 561		NZ	B 120	N4B	2.7	2.7	2.9	2.7
NZ	A 588	αC2	O	B 54	αN1	2.8	–	0	–
			OD2	C 44	N	–	3.1	0	2.8
O	D 589	αC2	N	D31 79	N2N3	–	–	–	3.0
OG	D 589		N	D31 80	N2N3	–	–	–	2.8
OG1	A 593	αC2	NE2	B 51	αN1	2.8	0	0	–

The first six columns show the name and secondary structure element of the interacting atoms. Helices and strands are preceded by "α" and "β," and the connecting loops are denoted by the names of the neighboring secondary structure elements (column SSE). The immunoglobulin domain is denoted "Im." For example, the first row indicates an interaction between the carbonyl oxygen of residue 105 in subunit A with the NH1 atom of residue 560 in subunit A51. The first atom is found in the loop between αN4 and βB, and the second in helix αC1. The last four columns show the distances between the atoms (in Å). Only distances shorter than 3.2 Å are listed. The headers of these columns show the label of the interacting subunits (Fig. 1 insert). A "–" denotes a missing interaction and a "0" denotes that one of the atoms is disordered. A putative magnesium ion is bridging one 5-fold and quasi-6-fold contact. A single water molecule at the 3-fold and quasi-3-fold axis is also included. Atoms belonging to the immunoglobulin and helical domains are shaded (helical domain light shading).

arginine side chains extend from the inner surface of the shell and two others are accessible on the inner surface but are involved in protein–protein contacts. The remaining four arginines are not exposed to the interior.

A divalent metal ion was modeled close to Asp207 and Asp182 in each subunit (Fig. 8). In subunits forming the flat contacts (D and B), the ion also binds to a main chain oxygen in the Ig domain of a quasi-6-fold-related subunit (C and D) (Fig. 4). The ion is present at the shell domains of A and C as well, although with weaker density. The bent contact causes the quasi-symmetry-related Ig-like domains (A and B) to be too far away for binding to the ion (Fig. 4). The distances between the oxygen atoms of the protein and the ion are about 2.4 Å, suggesting that the density is a divalent cation. Divalent ions often have six oxygen ligands and the remaining positions are probably occupied by

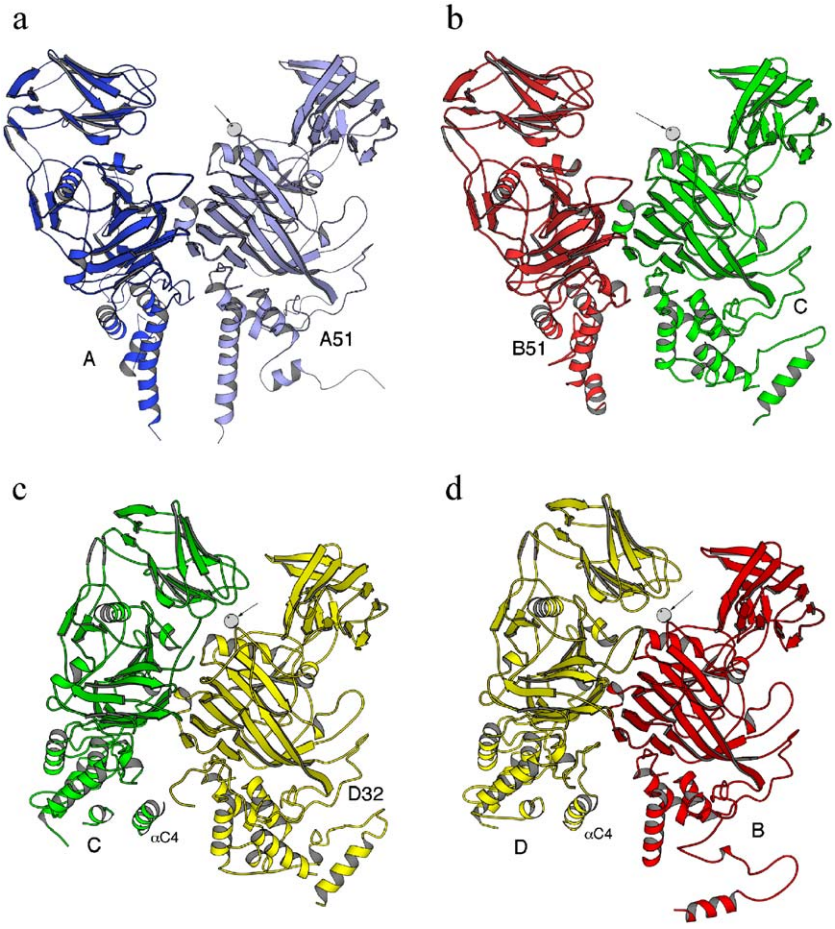

Fig. 4. The bent and flat contacts. (a) Two A subunits interacting around the 5-fold axis (bent). (b) B and C subunits around the quasi-6-fold axis (bent). (c) C and D subunits around the quasi-6-fold axis (flat). (d) D and B subunits around the quasi-6-fold axis (flat). Helix αC4 from the C and D subunits acts as a wedge, making the CD and DB dimer interactions flat. The location of the putative magnesium ions (gray ball) in each dimer interface is also shown.

occupied by poorly ordered water molecules. The electron density is similar to that of the protein and thus lower than what is expected for a calcium ion. It is therefore probably a magnesium ion. In several plant viruses, divalent cations are found in subunit–subunit interfaces and are important for the stabilization of the particles. The ion site in NωV, although found at an interface, is different in that it involves only a carbonyl oxygen from the immunoglobulin domain of one of the subunits. It is therefore probably not crucial for the stability of the particle.

Control of maturation

Virus-like particles formed by the expressed NωV protein form procapsids at neutral pH, and only after exposure to pH 5 undergo the maturation cleavage to produce the γ peptide (Canady et al., 2000, 2001). The lowering of the pH reduces the radius of the particle, and the shrinking and swelling is reversible in mutants that are deficient in cleavage. The arrangement of aspartate and glutamate residues at the bent quasi-2-fold contact might be important for the pH dependence of particle maturation. Fig. 5a shows the arrangement of Asp83, Asp85, Asp87, Glu110, and Asp124 on the surface of the A subunit. In the flat contact between C and D subunits, these residues are not involved in subunit–subunit interactions but interact with other parts of the N-terminus within the subunit. In the bent contact, some of these residues are in close contact. Carboxyl oxygens of Asp87 side chains related by the quasi-2-fold axis are at a distance of about 2.5 Å from each other, suggesting that at least one of them is protonated. The side chain of Glu110 is extended in the C and D subunits, but at the bent 2-fold contact, an extended conformation of the corresponding side chains in the A and B subunits is sterically impossible. The side chains are therefore bent and stacked on each other (Fig. 5b), which leads to a close contact (2.4–2.5 Å) between one of their carboxyl oxygens and an oxygen in the Asp124 side chain of the same subunit. There are thus four carboxylate groups in a very close arrangement. There is a histidine side chain close to Glu110, and the amino group of Lys113 is at a distance of 3.6–3.8 Å from Glu110. An image reconstruction of electron micro-

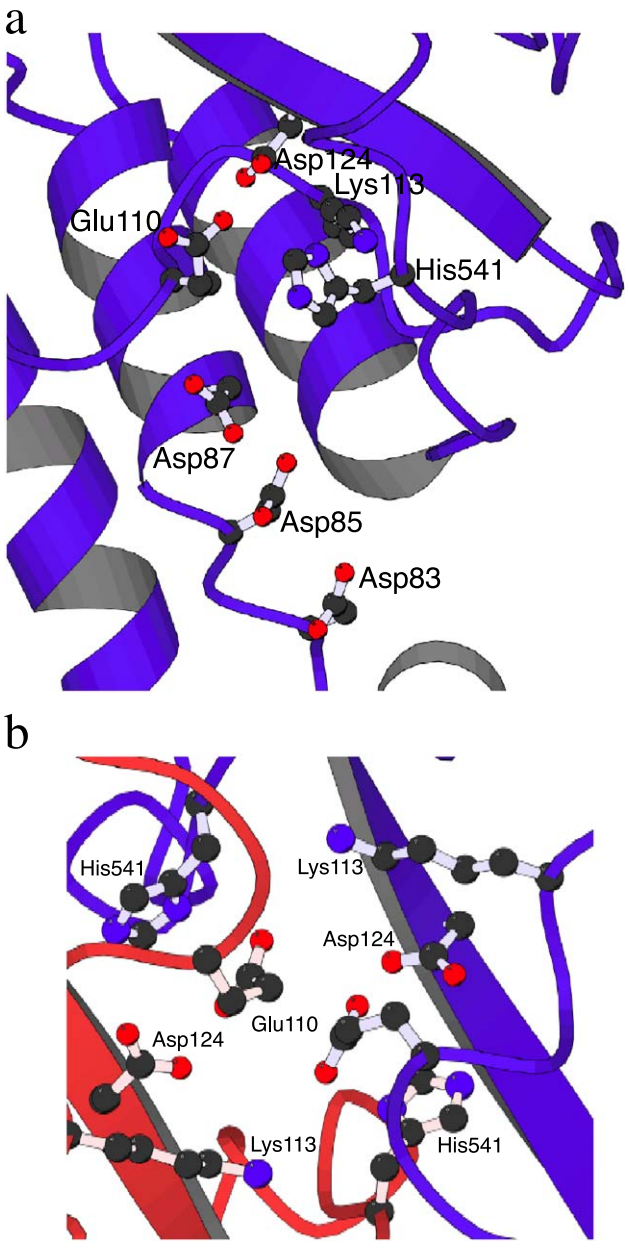

Fig. 5. Ten negative charges in the AB quasi-2-fold interface. The A subunit is blue and the B subunit is red. (a) The interface of the A subunit seen perpendicular to the quasi-2-fold axis. (b) The close contact of Glu110 and Asp124 as seen down the axis.

graphs of procapsid particles suggests that the dimeric interactions at both quasi-2-fold axes are closely similar, resembling those at the flat contact of the mature capsids (Canady et al., 2000). The carboxylate side chains therefore do not appear to be in close contact in the procapsid. At a neutral pH, all the aspartate and glutamate side chains will be unprotonated and charged and it is therefore unlikely that the bent contact can form. Upon lowering of the pH, some of the residues probably become protonated, allowing the bent contact to form. In the capsids, the pK_a of these carboxylate groups will be shifted from their normal value of about 4 due to their close proximity. When the pH is increased, the side chains will tend to be deprotonated, causing the particles to expand to the procapsid form.

It remains to explain why the maturation cleavage occurs only at low pH and why cleavage prevents the reexpansion of particles at neutral pH. The proposed mechanism for the autocatalytic cleavage (Taylor et al., 2002) does not require a low pH. It is therefore likely that the conformational changes that occur upon lowering the pH are responsible for the activation. Although the residues suggested to be directly involved in the catalysis reside in the same subunit as the cleaved bond, it is still possible that the subunit–subunit interactions in the low pH form of the capsids are important. Stabilization of residues involved in a mechanism is often important for catalysis. In the capsids, the cleavage site is to a large extent buried by neighboring subunits, and this may stabilize the active conformation of the residues involved in the cleavage. In the procapsid, these will be more flexible preventing the cleavage. Further, in the mature capsids, the Phe571 side chain at the N-terminus of the γ peptide form hydrophobic contacts with N-terminal regions from two other subunits. It is therefore possible that favorable packing of this side chain is necessary for the cleavage, and this will occur only when the subunits are interacting closely as in the low pH form. The contacts of the phenylalanine side chains might also explain the unexpected amino acid sequence at the cleavage site. The cleavage is expected to be more efficient if the amino acid after the active asparagines has a small side chain (Stephenson and Clarke, 1989). In the nodaviruses, the corresponding residue is an alanine and in the betatetravirus genus of the tetraviruses, the residue is a glycine. The interactions of the phenylalanine side chain might prevent it from interfering with the reaction.

In the absence of the cleavage, the particles reexpand at neutral pH. After the cleavage, this process might be prevented by favorable interactions that are formed only after cleavage. The released termini are rearranged, and several contacts are formed. The only direct subunit–subunit contacts involving the released termini is the hydrophobic interactions of Phe571 described above. It is possible that other stabilizing contacts are formed due to rearrangements that are possible only after the cleavage.

The role of the helix bundle in membrane translocation

A helix bundle formed by the γ peptides around the 5-fold axes in FHV was suggested to function in membrane translocation of the RNA (Cheng et al., 1994). The helix bundle could become attached to the cellular membrane and serve as mechanism for transporting the RNA into the cytoplasm. Biochemical studies and the crystallographic and EM structures of FHV support this hypothesis. The γ peptides close to the 5-fold axes form a helix bundle inside the particle (Fisher and Johnson, 1993). The part of the bundle facing the capsid center is associated with the genomic RNA (Cheng et al., 1994). The γ peptides can be removed from the otherwise intact particle by treatment

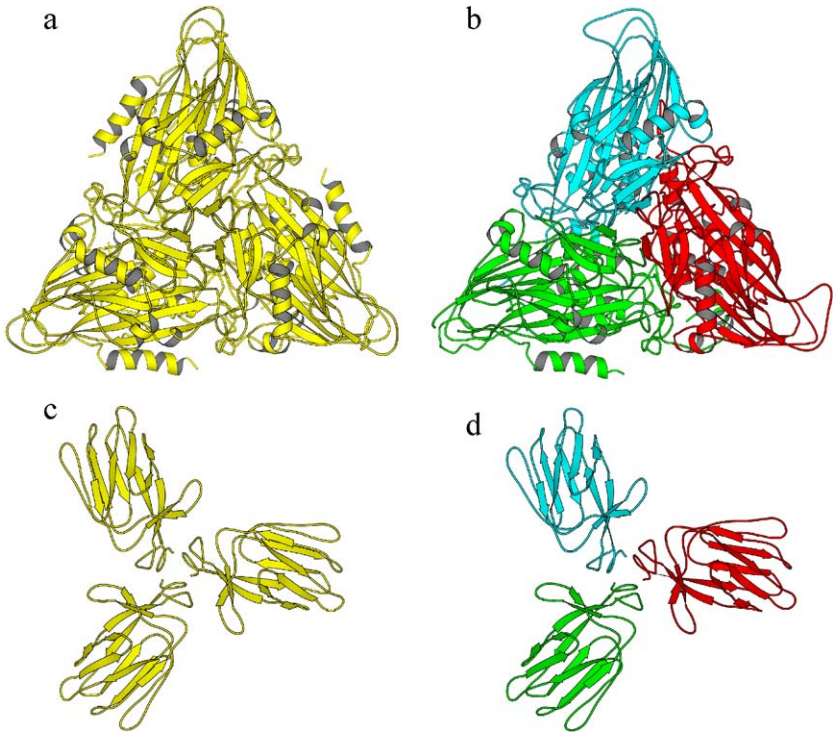

Fig. 6. The 3-fold and quasi-3-fold contacts. (a) The shell domains of three D subunits around the 3-fold axis. (b) The shell domains of A, B, and C subunits around the quasi-3-fold axis. (c) The Ig-like domains of three D subunits around the 3-fold axis. (d) The Ig-like domains of A, B, and C subunits around the quasi-3-fold axis.

with 1% (v/w) SDS (Gallagher and Rueckert, 1988), and a small portion of the genomic RNA is released from the capsid when exposed to heat followed by low pH (Cheng et al., 1994). The inside of the bundle is lined with polar residues, but the outside of the bundle is mainly hydrophobic, which would allow insertion into or association with the

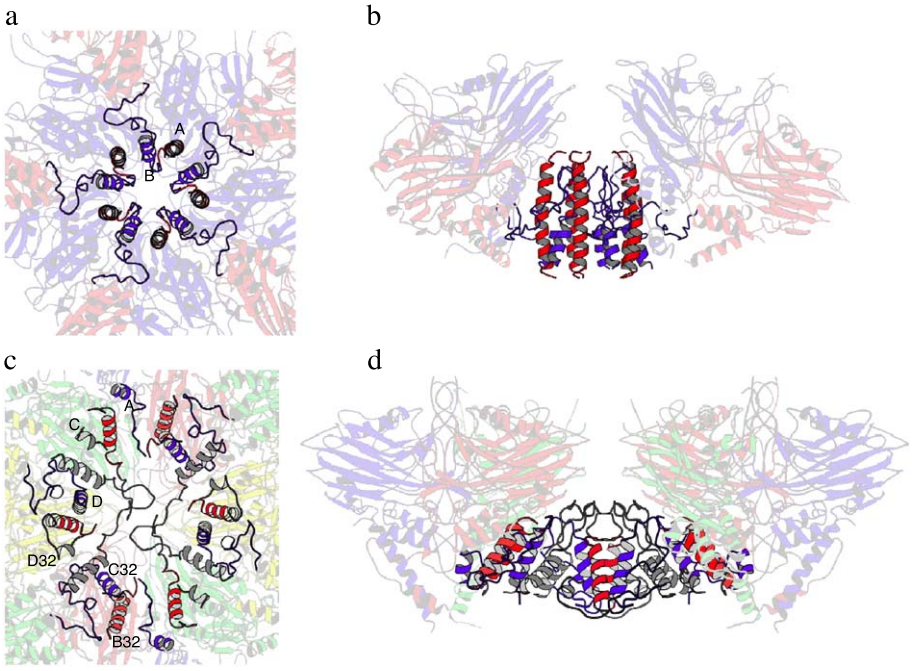

Fig. 7. Organization of the γ peptides. The γ peptides, αN1 and linker are in dark colors, the rest of the proteins are in pale colors. The N-terminal helices are in blue, the αC2 helices are red, and the αC3 and αC4 helices in the C and D subunits are grey. (a) The γ peptides (αC2 of the A subunit) and the C-terminal helices (αN1 of the B subunit) around the 5-fold axis. (b) The same as in a, but side view. (c) The γ peptides (αC2–αC4 of the C and D subunits, αC2 of the B subunit) and the N-terminal helices (αN1 of the A and C subunits) around the quasi-6-fold axis. (d) The same as in c, but side view.

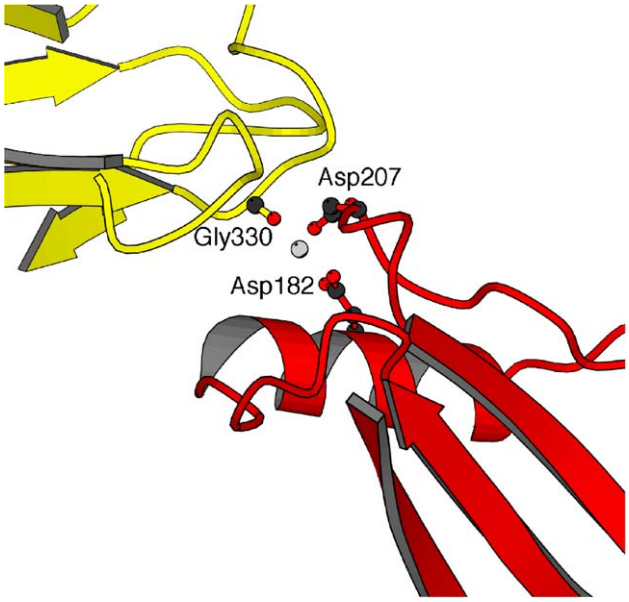

Fig. 8. Detailed interactions of the Mg^{2+}ion at the flat contact between subunits C and D.

cell membrane (Fisher and Johnson, 1993). The surface of the FHV capsid has a hydrophobic patch at the 5-fold axis that would allow the particle to make contact with the membrane (Fisher and Johnson, 1993). A density interpreted as a pocket factor in a cavity at the 5-fold axis could be released upon interaction and destabilize the capsid (Cheng et al., 1994). The residues surrounding the 5-fold axis are hydrophobic, which would allow the bundle to "slide out" following a structural change (Fisher and Johnson, 1993). Recently, it was demonstrated that sequences corresponding to residues 364–386 of the γ peptide of FHV are membrane active and readily form pores that release dyes from liposomes (Bong et al., 1999; Janshoff et al., 1999).

In NωV, the γ peptide is also cleaved off during maturation and this cleavage is necessary to stabilize the mature conformation (Taylor et al., 2002). There are, however, some differences in the helix bundle when compared to FHV. The γ peptides in NωV are considerably longer (571–644, 74 residues) than in FHV and BBV (364–407, 44 residues). The γ peptides at the 5-fold axis do not form a five-membered helical bundle as previously reported (Munshi et al., 1996). Instead, the γ peptides from the A chain are intercalated by five N-terminal helices, αN1, from the five neighboring B chains (Figs. 7a and b). The resulting 10-helix bundle is thus covalently attached to the rest of the capsid protein through the αN1 helices. To become completely externalized, the helix bundle must move approximately 75 Å radially outwards in the particle. The αN1 helix of the B subunit is followed by a long (residues 58–86) stretch of polypeptide that does not have any secondary structure and could be used as a linker to allow some movement of the helix bundle. This linker, however, is attached approximately in the middle of the bundle, which would be far away from the particle surface after externalization. If the bundle is completely externalized in its present conformation, the linker should be lining the outside of the bundle. The distance the linker would need to reach is approximately 90 Å, which is close to the maximum distance that 30 residues could span. The 10 helices do form a large, pore-like structure with an inner diameter of 20 Å, but as opposed to FHV, the inside of the pore is lined with hydrophobic residues and the outside is mainly polar (Fig. 9). A cavity lined with mostly hydrophobic residues is present at the 5-fold axis, between the bundle and the BC and DE loops facing to surface of the particle, but there is no evidence of a pocket factor. It is difficult to imagine the 10-helix bundle becoming externalized, and if it does it could not possibly be inserted into the membrane in its present form.

Methods

Model building and refinement

The crystallization, structure determination, and first high-resolution model of *N. capensis* ωVirus was published (Cavarelli et al., 1991; Munshi et al., 1996, 1998). The space group is P1 with one particle in the unit cell and 60-fold non-crystallographic symmetry. The data et used for refinement was collected on film and consisted of 2465275 independent reflections. The completeness was 51% and the scaling *R* factor 0.121. Using the program O (Jones et al., 1991), the model was partly rebuilt and several new

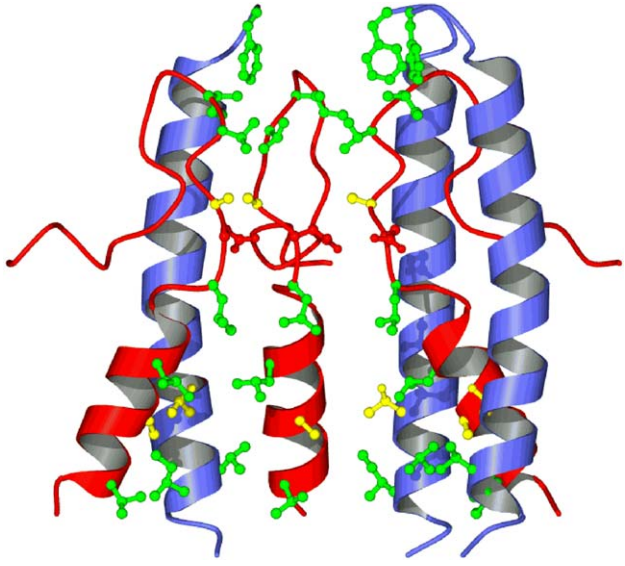

Fig. 9. The hydrophobic residues inside the helix bundle. Helices αC2 of the A subunit and αN1 of the B subunit from three different 5-fold-related asymmetric units are shown. Hydrophobic side chains in green, small side chains in yellow, and negatively charged side chains in red.

stretches of polypeptide were added. At one loop region, C141–C144, the density was too weak to allow modeling of the main chain, and these four residues were removed from the model. Maps were calculated and the phases were improved by cyclic averaging with the program Ave (Jones, 1992; Kleywegt and Jones, 1994). The model was refined by simulated annealing and conjugate gradient minimization with the program CNS (Brünger et al., 1998). The non-crystallographic symmetry was used as a constraint in the refinement. Refinement of temperature factors for individual atoms or groups of atoms in each residue lead to unrealistic values for many residues, and a temperature factor was therefore refined for each amino acid residue. The final R value is 22.0%. The free R value is very similar (22.2%) as is normal for the case of high non-crystallographic symmetry. The protein monomers consists of 644 residues, present in four different conformations, A, B, C, and D in the $T = 4$ shell. The final model includes residues A61–A599, B44–B590, C42–C140, C145–C590, C593–C601, C606–C641, D43–D601, D614–D641 (Fig. 3), four divalent metal ions modeled as Mg^{2+}, and 510 water molecules. The model and structure factors have been deposited in the Protein Data Bank (entry 1ohf).

Acknowledgments

This work was supported by The Swedish Research Council, the Swedish foundation for Strategic Research and NIH Grant GM54076. Derek Taylor and Kelly Lee have made useful comments to the manuscript.

References

Bong, D.T., Steinem, C., Janshoff, A., Johnson, J.E., Reza Ghadiri, M., 1999. A highly membrane-active peptide in Flock House virus: implications for the mechanism of nodavirus infection. Chem. Biol. 6 (7), 473–481.

Brünger, A.T., Adams, P.D., Clore, G.M., DeLano, W.L., Gros, P., Grosse-Kunstleve, R.W., Jiang, J.-S., Kuszewski, J., Nilges, M., Pannu, N.S., Read, R.J., Rice, L.M., Simonson, T., Warren, G.L., 1998. Crystallography and NMR system: a new software suite for macromolecular structure determination. Acta Crystallogr., Sect. D 54, 905–921.

Canady, M.A., Tihova, M., Hanzlik, T.N., Johnson, J.E., Yeager, M., 2000. Large conformational changes in the maturation of a simple RNA virus, *Nudaurelia capensis* ω virus (NωV). J. Mol. Biol. 299, 573–584.

Canady, M.A., Tsuruta, H., Johnson, J.E., 2001. Analysis of rapid, large-scale protein quaternary structural changes: time-resolved X-ray solution scattering of *Nudaurelia capensis* omega virus (NomegaV) maturation. J. Mol. Biol. 311 (4), 803–814.

Cavarelli, J., Bomu, W., Liljas, L., Kim, S., Minor, W., Munshi, S., Muchmore, S., Schmidt, T., Johnson, J.E., 1991. Crystallization and preliminary structure analysis of an insect virus with $T = 4$ quasi-symmetry: *Nudaurelia capensis* ω Virus. Acta Crystallogr. B47, 23–29.

Cheng, R.H., Reddy, V.S., Olson, N.H., Fisher, A.J., Baker, T.S., Johnson, J.E., 1994. Functional implications of quasi-equivalence in a $T = 3$ icosahedral animal virus established by cryo-electron microscopy and X-ray crystallography. Structure 2, 271–282.

Fisher, A.J., Johnson, J.E., 1993. Ordered duplex RNA controls capsid architecture in an icosahedral animal virus. Nature 361, 176–179.

Gallagher, T.M., Rueckert, R.R., 1988. Assembly-dependent maturation cleavage in provirions of a small icosahedral insect ribovirus. J. Virol. 62, 3399–3406.

Hosur, M.V., Schmidt, T., Tucker, R.C., Johnson, J.E., Gallagher, T.M., Selling, B.H., Rueckert, R.R., 1987. Structure of an insect virus at 3.0 Å resolution. Proteins: Struct. Funct. Genet. 2, 167–176.

Janshoff, A., Bong, D.T., Steinem, C., Johnson, J.E., Ghadiri, M.R., 1999. An animal virus-derived peptide switches membrane morphology: possible relevance to nodaviral transfection processes. Biochemistry 38 (17), 5328–5336.

Jones, T.A., 1992. CCP4 Study Weekend 1992: Molecular Replacement, Daresbury, England.

Jones, T.A., Zou, J.-Y., Cowan, S.W., Kjeldgaard, M., 1991. Improved methods for building protein models in electron density maps and the location of errors in these models. Acta Crystallogr. A47, 110–119.

Kleywegt, G.J., Jones, T.A., 1994. Halloween ... Masks and Bones. In: Bailey, S., Hubbard, R., Waller, D. (Eds.), From First Map to Final Model. Proceedings of the CCP4 Study Weekend. SERC Daresbury Laboratory, Daresbury, pp. 59–66.

Kleywegt, G.J., Jones, T.A., 1996. Phi/psi-chology: Ramachandran revisited. Structure 4, 1395–1400.

Kraulis, P.J., 1991. Molscript: a program to produce both detailed and schematic plots of protein structures. J. Appl. Crystallogr. 24, 946–950.

Laskowski, R.A., MacArthur, M.W., Moss, D.S., Thornton, J.M., 1993. PROCHECK: a program to check the stereochemical quality of protein structures. J. Appl. Crystallogr. 26, 283–291.

Munshi, S., Liljas, L., Cavarelli, J., Bomu, W., McKinney, B., Reddy, V., Johnson, J.E., 1996. The 2.8 Å resolution structure of a $T = 4$ animal virus and its implications for membrane translocation of RNA. J. Mol. Biol. 261, 1–10.

Munshi, S., Liljas, L., Johnson, J.E., 1998. The structure determination of *Nudaurelia capensis* ω Virus. Acta Crystallogr. D54, 1295–1305.

Stephenson, R.C., Clarke, S., 1989. Succinimide formation from aspartyl and asparaginyl peptides as a model for the spontaneous degradation of proteins. J. Biol. Chem. 264, 6164–6170.

Tang, L., Johnson, K.N., Ball, L.A., Lin, T., Yeager, M., Johnson, J.E., 2001. The structure of pariacoto virus reveals a dodecahedral cage of duplex RNA. Nat. Struct. Biol. 8, 77–83.

Taylor, D.J., Krishna, N.K., Canady, M.A., Schneemann, A., Johnson, J.E., 2002. Large-scale, pH-dependent, quaternary structure changes in an RNA virus capsid are reversible in the absence of subunit autoproteolysis. J. Virol. 76, 9972–9980.

Wery, J.-P., Reddy, V.S., Hosur, M.V., Johnson, J.E., 1994. The refined three-dimensional structure of an insect virus at 2.8 Å resolution. J. Mol. Biol. 235, 565–586.

Wynne, S.A., Crowther, R.A., Leslie, A.G., 1999. The crystal structure of the human hepatitis B virus capsid. Mol. Cell 3, 771–780.